An Organic Solid State Injection Laser

J. H. Schön, *et al.*

Science **289**, 599 (2000);
DOI: 10.1126/science.289.5479.599

Science (print ISSN 0036-8075; online ISSN 1095-9203) is published weekly, except the last week in December, by the American Association for the Advancement of Science, 1200 New York Avenue NW, Washington, DC 20005.

Sup35p is at least 20-fold less than that of ribosomes, which are present at ~200,000 copies per yeast cell. See (*35*) for an estimate of ribosomes per yeast cell and (*36*, *37*) for a quantification of Sup35p relative to ribosomes.
26. H. E. Sparrer, A. Santoso, F. C. Szoka Jr., J. S. Weissman, unpublished data.
27. Y. O. Chernoff, S. L. Lindquist, B.-i. Ono, S. G. Inge-Vechtomov, S. W. Liebman, *Science* **268**, 880 (1995).
28. M. F. Tuite, C. R. Mundy, B. S. Cox, *Genetics* **98**, 691 (1981).
29. In preliminary experiments, we addressed the role of the [*pin*] element in yeast, which is an epigenetic modifier, that facilitates the formation of [*PSI*$^+$] (*38*). We found that a stable [*PSI*$^+$] state could also be introduced into an otherwise isogenic [*pin*$^-$] strain of 74D-694, but the rate of conversion decreased substantially in the absence of [*PIN*$^+$] factor. This is consistent with the proposal that the [*PSI*$^+$] phenotype can be induced and propagated independently of [*PIN*$^+$], but that [*PIN*$^+$] facilitates [*PSI*$^+$] formation (*39*).
30. Y. O. Chernoff, I. L. Derkach, S. G. Inge-Vechtomov, *Curr. Genet.* **24**, 268 (1993).
31. I. L. Derkatch, M. E. Bradley, S. W. Liebman, *Proc. Natl. Acad. Sci. U.S.A.* **95**, 2400 (1998).
32. G. P. Newnam, D. R. Wegrzyn, S. L. Lindquist, Y. O. Chernoff, *Mol. Cell. Biol.* **19**, 1325 (1999); S. Krobitsch, S. L. Lindquist, *Proc. Natl. Acad. Sci. U.S.A.* **97**, 1589 (2000).
33. Y. O. Chernoff, G. P. Newnam, J. Kumar, K. Allen, A. D. Zink, *Mol. Cell. Biol.* **19**, 8103 (1999).
34. M. D. Michelitsch and J. S. Weissman, in preparation.
35. J. R. Warner, *Trends Biochem. Sci.* **24**, 437 (1999)
36. S. A. Didichenko, M. D. Ter-Avanesyan, V. N. Smirnov, *Eur. J. Biochem.* **198**, 705 (1991).
37. I. Stansfield, C. M. Grant, Akhmaloka, M. F. Tuite, *Mol. Microbiol.* **6**, 3469 (1992).
38. I. L. Derkatch, M. E. Bradley, P. Zhou, Y. O. Chernoff. S. W. Liebman, *Genetics* **147**, 507 (1997).
39. I. L. Derkatch *et al.*, *EMBO J.* **19**,1942 (2000).
40. F. Szoka Jr. *et al.*, *Proc. Natl. Acad. Sci. U.S.A.* **78**, 1685 (1981).
41. We thank L. Gagne and M. Springer for assistance in liposome preparation and microscopy and F. E. Cohen, P. S. Kim, E. O'Shea, and members of the Lim and Weissman lab for helpful discussions. Supported by the NIH, the Searle Scholars Program, the David and Lucile Packard Foundation, and a postdoctoral fellowship from the European Molecular Biology Organization (H.E.S.).

15 March 2000; accepted 9 June 2000

An Organic Solid State Injection Laser

J. H. Schön, Ch. Kloc, A. Dodabalapur, B. Batlogg*

We report on electrically driven amplified spontaneous emission and lasing in tetracene single crystals using field-effect electrodes for efficient electron and hole injection. For laser action, feedback is provided by reflections at the cleaved edges of the crystal resulting in a Fabry-Perot resonator. Increasing the injected current density above a certain threshold value results in the decreasing of the spectral width of the emission from 120 millielectron volts to less than 1 millielectron volt because of gain narrowing and eventually laser action. High electron and hole mobilities as well as balanced charge carrier injection lead to improved exciton generation in these gate-controlled devices. Moreover, the effect of charge-induced absorption is substantially reduced in high-quality single crystals compared with amorphous organic materials.

Semiconductor lasers are widely used in modern science and technology. Compared with conventional inorganic semiconductors, organic semiconductors offer potential advantages with respect to easy processing, lower cost, and flexibility. Hence, electrically driven lasers based on organic semiconductors might find a wide range of applications. Optically excited lasing and amplified spontaneous emission have been observed in a wide range of semiconducting polymers, small molecules, and organic single crystals (*1*–*9*). Moreover, amorphous or nearly amorphous organic and polymeric semiconductors have been very successfully used in thin-film organic light-emitting devices (OLEDs). These devices typically require injection current densities of 1 to 10 mA/cm^2 to achieve brightnesses of order 100 cd/m^2 (*4*). For laser applications, substantially higher current densities will be required. Reduced luminescence efficiencies at high injection current densities and charge-induced absorption have been identified as major problems for electrically pumped OLEDs (*4*, *10*, *11*). Another limiting factor is the low charge carrier mobility. As an electrically driven device is strongly influenced by the transport properties of the semiconductor, we focus on organic materials that exhibit high mobilities for electrons as well as holes.

Materials properties. Mobilities on the order of 2 cm^2 V^{-1} s^{-1} can be achieved in tetracene at room temperature. This is more than four orders of magnitude higher than mobilities in materials used in conventional OLEDs (*4*, *8*, *10*). Tetracene also offers a reasonably high photoluminescence quantum yield, and electroluminescence has been reported for single-crystal diodes (*12*). Optically pumped amplified spontaneous emission has been observed in tetracene-doped (*13*, *14*) and undoped anthracene single crystals (*15*). To minimize extrinsic influences such as grain boundaries, defects, or disorder, we investigated high-quality single crystalline samples to unveil the intrinsic opto-electronic properties of this material.

Device design. To ensure facile electrical contacts and balanced injection of electrons and holes, we used two field-effect electrodes. Tetracene single crystals were grown from the vapor phase in a stream of inert gas (*16*). Typical samples exhibit smooth faces of some mm^2 and thicknesses in the range of about 1 to 10 μm. Field-effect device structures were prepared on freshly cleaved crystal surfaces. Source and drain electrodes (Au for holes and Al for electrons, respectively) were thermally evaporated through a shadow mask defining a 25-μm channel length and several hundred μm channel width. An amorphous Al_2O_3 layer was sputtered onto the crystal, resulting in a capacitance of C_i = 50 nF/cm^2 between the gate electrode and the crystal. Finally, transparent Al-doped ZnO gate electrodes were deposited. A schematic of the structure is shown in Fig. 1A.

It has been recently demonstrated that ambipolar charge transport, i.e., n- as well as p-channel activity, can be obtained in high-quality single-crystal polyacene field-effect transistors (FETs) (*17*). Hence, gate-controlled electrodes can realize efficient electron as well as hole injection, with the field-induced charge acting as a heavily doped "contact" to the crystal. Furthermore, charge carrier mobilities as high as 10^3 to 10^5 cm^2 V^{-1} s^{-1} are achieved at low temperatures, and Fractional Quantum Hall transport has been observed in similar devices at temperatures below 4 K (*18*). Typical threshold voltages V_t of the FETs are −0.6 V for p-channel and +1 V for n-channel operation. The carrier concentration in the channel region can be adjusted by the applied gate voltage. Organic semiconductor crystals can act as a waveguide, as has been shown for optically pumped oligothiophene crystals (*19*, *20*). However, in the present structure, the Al_2O_3 layer (~150 nm) is too thin to serve as a cladding layer. Thus, a planar multimode waveguide is formed by the entire structure with air as the cladding material on both sides. This means that at low injection current densities, a substantial fraction of the guided modes are in the lossy ZnO layers. The geometry of the device is such that there are many modes, and an analysis of the optics of this structure will be published elsewhere. An overall internal loss on the order of 100 cm^{-1} is estimated for this multilayer structure. Feedback is provided by cleaving the crystal perpendicular to the waveguide structure, resulting in a Fabry-Perot–type resonator. Assuming an ideal reflectivity of 8% for these cleaved edges, mirror losses on the order of 50

Bell Laboratories, Lucent Technologies, 600 Mountain Avenue, Murray Hill, NJ 07974–0636, USA.

*To whom correspondence should be addressed. E-mail: batlogg@lucent.com

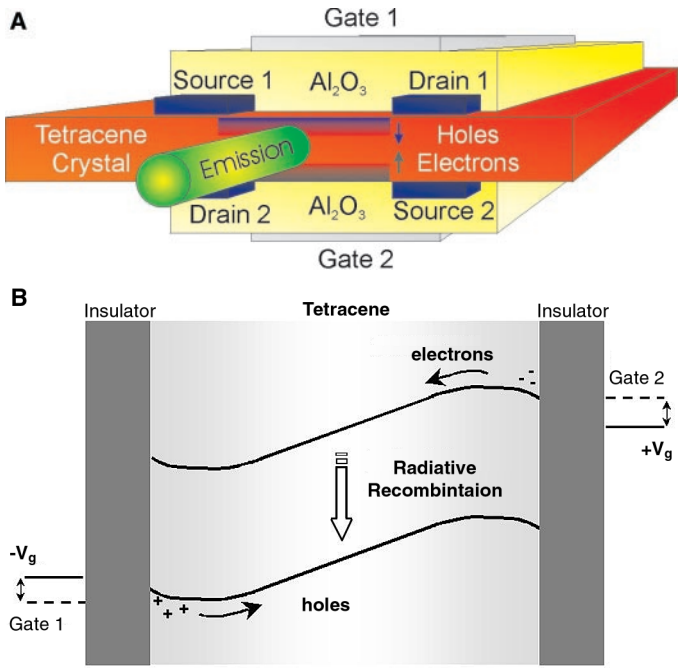

Fig. 1. (**A**) Structure of the tetracene single-crystal device that uses two field-effect electrodes for charge injection. Source, drain electrodes, a gate dielectric layer, and gate electrodes were deposited on the top and bottom of a single crystal. Electrons and holes are injected by applying a positive (bottom) or negative (top) source-gate voltage, respectively. In addition, a voltage (about 5 V) was applied across the crystal between both field-effect electrodes (between drain 1 and source 2 as well as between source 1 and drain 2). Electroluminescence and amplified stimulated emission are detected from the edge of the crystal. (**B**) Schematic energy band diagram illustrating the directions of electron and hole current flow in the device.

to 100 cm^{-1} are estimated for a resonator length of several hundred μm. However, we expect the actual reflectivity at the facets of the crystal to be lower than 8% because of imperfections in the cleaving. In such structures, it is expected that gain guiding becomes important at high injection current densities.

Device operation. Applying a negative gate voltage to the top gate and a positive voltage to the bottom gate, holes and electrons are induced at the top and bottom tetracene/Al_2O_3 interface, respectively. The electron (n_e) and hole (n_h) concentration can be estimated with the gate voltage V_g and capacitance C_i ($n \approx C_i V_g/e$). Densities on the order of 10^{13} cm^{-2} are achieved for V_g of 50 V. If a potential difference is applied between the electron gas and hole gas induced by the two gates, the electrons and holes will flow to the bottom and top, respectively, resulting in a net current across the device (Fig. 1B). This voltage, which represents the voltage drop in the sample, was maintained at 5 V in the experiments reported here. However, the current density is varied by the applied gate voltages. This changes the conductivity of the electron and hole gases that form the "ohmic contacts" to the bulk of the crystal. Thus, current injection into the device is essentially contact limited. As a result of the injection of electrons and holes, excitons are formed and light is emitted. The emission intensity at 5 K as a function of the pulsed current density (10 μs, 100 Hz) up to 1700 A/cm^2 (Fig. 2) shows that at relatively low current densities j (<1 A/cm^2), three peaks can be observed (see Fig. 3). They can be identified as radiative recombination from the first excited state to the ground state (0-0) and its vibronic progressions (0-1, 0-2, . . .) (*21*). The spacing between the bands of 170 meV corresponds to intramolecular vibrations. When the current density is increased by increasing the source-gate voltages, the 0-1 band becomes dominant and its width narrows from about 120 meV to 10 meV for 30 A/cm^2. Finally, at even higher j (>500 A/cm^2), the linewidth collapses to less than 1 meV (see Fig. 4) and is limited by the resolution of the measurement setup. The abrupt spectral narrowing in combination with the distinct threshold (30 A/cm^2) is typical of amplified spontaneous emission along with gain guiding. The second decrease of the linewidth at higher current densities (>500 A/cm^2) indicates the onset of laser action. The estimated gain becomes comparable to the overall resonator losses, resulting in laser action at these current densities. The large difference between thresholds for observing gain narrowing and laser action is because of the low reflectivities of the end mirrors, which lead to a high mirror loss.

Above the threshold for the amplification of spontaneous emission, Fabry-Perot fringes characteristic of a resonator with gain are observed. The fringe spacings are consistent with axial mode spacings of a cavity of appropriate length (*22*, *23*) (see Fig. 3 and insets in Fig. 2). The reduction in the number of peaks with increasing pump power is also a clear indication of laser action at current densities exceeding 500 A/cm^2. At the highest pump current densities, a single resolution limited peak is observed at 575.7 nm. The transition from amplified spontaneous emission to laser action occurs

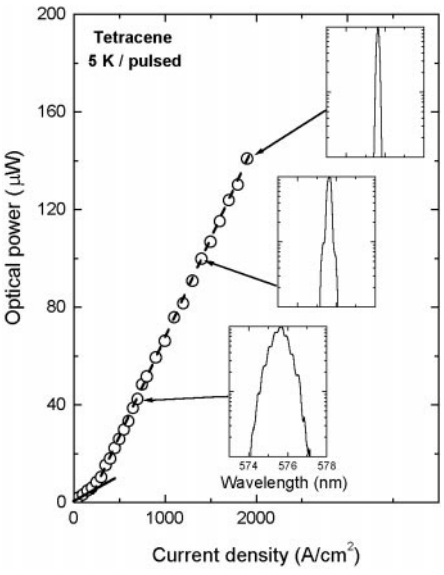

Fig. 2. Optical power as a function of current density for pulsed excitation (10 μs, 100 Hz) at 5 K. The insets show the change of the emission spectrum as a function of excitation.

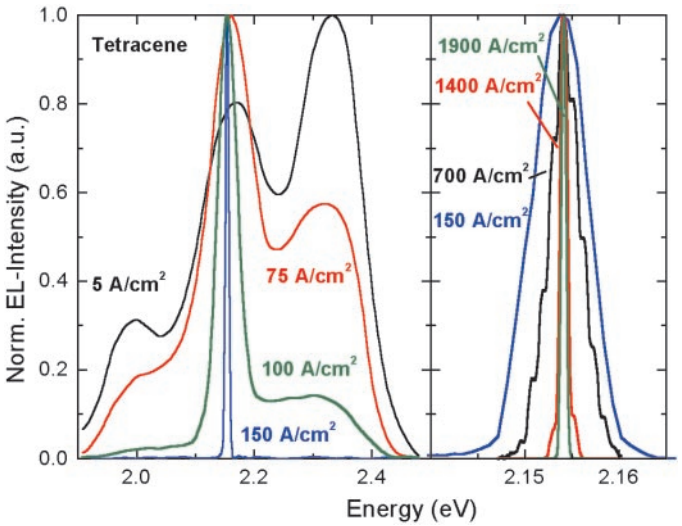

Fig. 3. Normalized electroluminescence (EL) intensity at 5 K as a function of energy for various current densities. The spectral narrowing of the 0-1 peak (at 2.15 eV) is visible. The right-hand picture shows the magnified spectral dependence for pulsed current densities exceeding 200 A/cm^2 on an expanded energy scale.

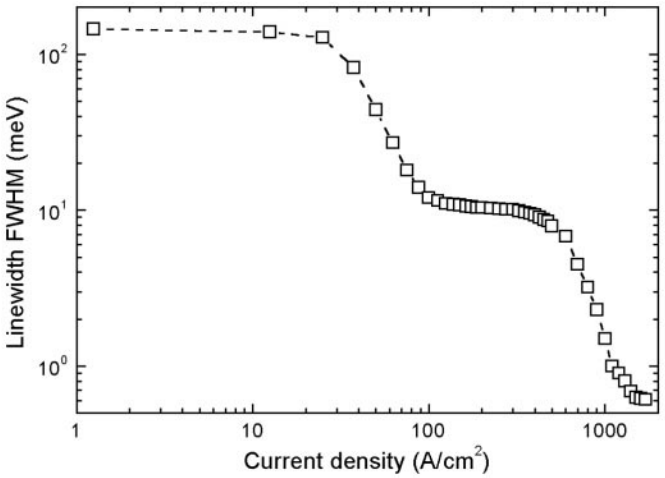

Fig. 4 (left). Full width at half maximum (FWHM) of the emission spectrum as a function of excitation current density (5 K, pulsed). The linewidth collapses from about 120 meV to less than 1 meV. At the highest current densities, the linewidth is limited by the resolution of the setup.

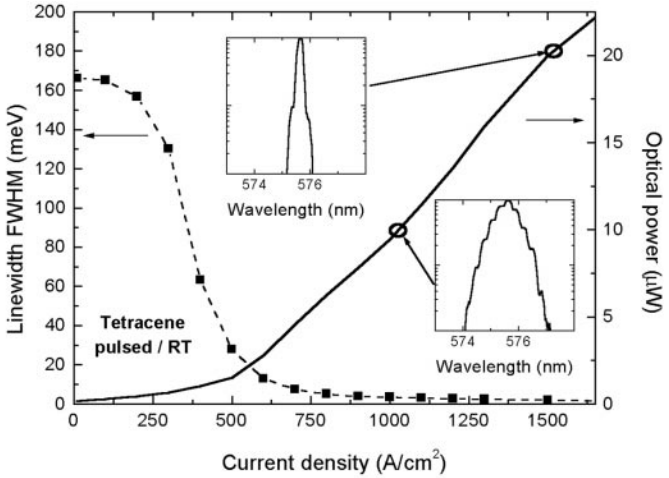

Fig. 5 (right). Optical power as a function of current density for pulsed excitation (10 μs, 100 Hz) at room temperature. The insets show the change of the emission spectrum as a function of excitation. RT, room temperature.

near 500 A/cm^2; this can also be discerned from the slopes in Fig. 2. As pointed out above, the threshold for observing effects of optical gain is much lower (~30 A/cm^2). Gain narrowing is also observed at low temperatures (<200 K) for continuous wave (CW) excitation. Emission spectra taken at 300 K are shown in the inset of Fig. 5 for pulsed excitation at two injection densities. Here again we observe signatures of amplified spontaneous emission and lasing, with a single peak above current densities of 1600 A/cm^2.

The use of two-dimensional gases of electrons and holes is an effective way to inject electrons and holes into a nominally undoped semiconductor. Doping of such semiconductors is possible and has been demonstrated. However, the diffusion of such dopants is likely to adversely affect the optical properties. Thus, the formation of electron and hole gases with field-effect structures is a promising way to realize efficient ohmic contacts to inject large carrier densities required for laser action in organic single crystals. We reiterate that while the source-gate voltage is being modulated, the potential difference across the organic crystal is held fixed at 5 V. In our arrangement, it is the source-gate voltage modulation that is responsible for the changes in intensity as well as gain narrowing of the emission spectra. Moreover, the injection of charge carriers can be controlled and balanced by individually adjusting the source-gate voltages of both metal-insulator-semiconductor structures. As the threshold voltage V_t was similar for the n- and p-channel FETs, the source-gate voltages were chosen to be the same for electron and hole injection.

Future prospects. Organic semiconductors can be approximated by a four-level system (*24*), unlike semiconductors such as GaAs, which are three-level systems. The natural stokes shift that exists between the absorption and emission spectra means that the threshold pump density required to achieve transparency is much less than in materials such as GaAs. Indeed, all that is required is to overcome the losses of the system. Optimization of the materials used in the structure shown in Fig. 1 will help lower the optical losses of the system. In amorphous OLEDs, carrier-induced transparency is overwhelmed by the induced absorption (*25*). In sharp distinction, in single crystals of tetracene, our data imply that the gain is higher than the combined losses—residual and carrier-induced. The above factor, as well as the much higher mobilities and transparencies near the absorption edge, are advantages of single crystals over amorphous and polycrystalline organic semiconductors for injection laser applications. Thus, although disordered organic/polymer semiconductors have proven to be very successful for light-emitting device applications, our results indicate that high-quality single crystals hold promise for injection lasers based on organic semiconductors.

The above inferences suggest that in an optimized device, the threshold current density (for laser action) could be more than two orders of magnitude less than the maximum injection density used in these experiments. This in turn indicates that room temperature CW-laser action is a strong possibility in materials such as tetracene. The structure used for this study can be improved upon in many ways to lower the threshold for stimulated emission. Use of a low-loss waveguide is an obvious way. The incorporation of a high-quality cavity or resonator will facilitate true room temperature CW-laser action by reducing the threshold.

References and Notes

1. N. Karl, *Phys. Status. Solidi (a)* **13**, 651 (1972).
2. F. Hide, M. A. Diaz-Garcia, A. J. Heeger, *Laser Focus World* **33** (no. 5), 151 (1997).
3. N. Tessler, G. J. Denton, R. H. Friend, *Laser Optoelektronik* **29**, 54 (1997).
4. N. Tessler, *Adv. Mater.* **11**, 363 (1999).
5. A. Dodabalapur *et al.*, *IEEE J. Sel. Top. Quant. Electr.* **4**, 67 (1998).
6. C. Zenz *et al.*, *Appl. Phys. Lett.* **71**, 2566 (1997).
7. C. Kallinger *et al.*, *Adv. Mater.* **10**, 920 (1998).
8. S. Frolov, M. Shkunov, A. Fujii, K. Yoshino, Z. V. Vardeny, *IEEE J. Quantum Electron.* **QE-36**, 2 (2000).
9. G. E. Jabbour *et al.*, *IEEE J. Quantum Electron.* **QE-36**, 12 (2000).
10. P. W. M. Blom and M. J. M. de Jong, *IEEE J. Sel. Top. Quant. Electr.* **4**, 105 (1998).
11. V. G. Kozlov *et al.*, *IEEE J. Quantum Electron.* **QE-36**, 18 (2000).
12. J. Kalinowski, J. Godlewski, R. Signerski, *Mol. Cryst. Liq. Cryst.* **33**, 247 (1976).
13. O. S. Avanesyan, V. A. Benderskii, V. Kh. Brikenstein, V. L. Broude, A. G. Lavrushko, *Phys. Status Solidi (a)* **19**, K121 (1973).
14. O. S. Avanesyan, V. A. Benderskii, V. Kh. Brikenshtein, A. G. Lavrushko, P. G. Filippov, *Phys. Status Solidi (a)* **30**, 781 (1975).
15. O. S. Avanesjan *et al.*, *Mol. Cryst. Liq. Cryst.* **29**, 165 (1974).
16. Ch. Kloc, P. G. Simpkins, T. Siegrist, R. A. Laudise, *J. Cryst. Growth* **182**, 416 (1997).
17. J. H. Schön, S. Berg, Ch. Kloc, B. Batlogg, *Science* **287**, 1022 (2000).
18. J. H. Schön, Ch. Kloc, B. Batlogg, *Science*, in press.
19. D. Fichou, S. Delysse, J.-M. Nunzi, *Adv. Mater.* **9**, 1178 (1997).
20. F. Garnier, G. Horowitz, P. Valat, F. Kouki, V. Wintgens, *Appl. Phys. Lett.* **72**, 2087 (1998).
21. D. D. Kolendritskii, M. V. Kurik, Y. P. Piryatinskii, *Opt. Spectrosc. (USSR)* **44**, 162 (1978).
22. R. J. Nelson, R. B. Wilson, P. D. Wright, P. A. Barnes, N. Y. Dutta, *IEEE J. Quantum Electron.* **QE-17**, 202 (1981).
23. T. P. Lee, C. A. Burrus, J. A. Copeland, A. G. Dentai, D. Marcuse, *IEEE J. Quantum Electron.* **QE-18**, 1101 (1982).
24. M. Berggren, A. Dodapalapur, R. E. Slusher, *Appl. Phys. Lett.* **71**, 2230 (1997).
25. V. G. Kozlov, P. E. Burrows, G. Parthasarathy, S. R. Forrest, *Appl. Phys. Lett.* **74**, 1058 (1999).
26. We thank F. Capasso, E. A. Chandross, S. V. Frolov, and R. E. Slusher for helpful discussions; O. Schenker for technical assistance; and E. Bucher for use of equipment. Furthermore, one of the authors (J.H.S.) gratefully acknowledges financial support by the Deutsche Forschungsgemeinschaft.

14 June 2000; accepted 4 July 2000

Retraction

WE ARE WRITING AS COAUTHORS ON THE following manuscripts published in *Science*, which were, in part, the subject of an independent investigation conducted at the behest of Bell Laboratories, Lucent Technologies. The independent committee reviewed concerns related to the validity of data associated with the device measurements described in the papers.

1) J. H. Schön, S. Berg, Ch. Kloc, B. Batlogg, Ambipolar pentacene field-effect transistors and inverters, *Science* **287**, 1022 (2000).

2) J. H. Schön, Ch. Kloc, R. C. Haddon, B. Batlogg, A superconducting field-effect switch, *Science* **288**, 656 (2000).

3) J. H. Schön, Ch. Kloc, B. Batlogg, Fractional quantum Hall effect in organic molecular semiconductors, *Science* **288**, 2338 (2000).

4) J. H. Schön, Ch. Kloc, A. Dodabalapur, B. Batlogg, An organic solid state injection laser, *Science* **289**, 599 (2000).

5) J. H. Schön, A. Dodabalapur, Ch. Kloc, B. Batlogg, A light-emitting field-effect transistor, *Science* **290**, 963 (2000).

6) J. H. Schön, Ch. Kloc, H. Y. Hwang, B. Batlogg, Josephson junctions with tunable weak links, *Science* **292**, 252 (2001).

7) J. H. Schön, Ch. Kloc, B. Batlogg, High-temperature superconductivity in lattice-expanded C_{60}, *Science* **293**, 2432 (2001).

8) J. H. Schön, H. Meng, Z. Bao, Field-effect modulation of the conductance of single molecules, *Science* **294**, 2138 (2001).

As a result of the committee's findings, we feel obligated to the scientific community to issue a retraction of the above articles. We note that although these papers may contain some legitimate ideas and contributions, we think it best to make a complete retraction.

ZHENAN BAO,[1] BERTRAM BATLOGG,[2] STEFFEN BERG,[3] ANANTH DODABALAPUR,[4] ROBERT C. HADDON,[5] HAROLD HWANG,[1] CHRISTIAN KLOC,[1] HONG MENG,[6] J. HENDRIK SCHÖN[7]

[1]Bell Laboratories, Lucent Technologies, 600 Mountain Avenue, Murray Hill, NJ 07974, USA. [2]Solid State Physics Laboratory, Eidgenössische Technische Hochschule, CH-8093 Zurich, Switzerland. [3]Max-Planck-Institut für Polymerforschung, D-55021 Mainz, Germany. [4]Microelectronics Research Center, University of Texas, Austin, TX 78758, USA. [5]Department of Chemistry, University of California, Riverside, 900 University Avenue, Riverside, CA 92521–0403, USA. [6]Department of Chemistry and Biochemistry, University of California, Los Angeles, 607 Charles E. Young Drive East, Los Angeles, CA 90095–1569, USA. [7]Summit, NJ, USA.

Editor's Note: For more information on the investigation, please see the summary and full report of the committee, which are available at www.lucent.com/news_events/researchreview.html.

The Origin of a Most Contentious Rock

IN "METASOMATIC ORIGIN OF QUARTZ-pyroxene rock, Akilia, Greenland and implications for Earth's earliest life" (Reports, 24 May, p. 1448), C. M. Fedo and M. J. Whitehouse conclude that rocks previously interpreted as metamorphosed sedimentary banded iron formation (BIF) and thought to contain the oldest evidence of life are instead highly deformed and metasomatized ultramafic igneous rocks. This conclusion is based, in part, on a comparison of trace element characteristics in the banded quartz-pyroxene rocks and various mafic and ultramafic igneous rocks. Unfortunately, data for only one of the ten banded rocks analyzed are shown in all of their chemical discrimination diagrams (Fig. 3). Although this one sample (AK 38) is consistent with the hypothesis, data for the nine remaining samples are very different and reveal it to be a misleading "proxy for the entire quartz-pyroxene lithology" as stated. Indeed, ratios of Th/Sc, Cr/Th, Cr/Y, and TiO_2/P_2O_5 in the nine samples overlap those reported for the Isua BIF and are distinct from those in ultramafic rocks. It is unlikely that a combination of metasomatic gains and losses could have produced such a match. Given that the origin of banding in these rocks is equivocal and that some elemental data (rare earth element) are incompatible with either an ultramafic or BIF precursor, ratios of the least mobile trace elements would seem to be an appropriate means to constrain protolith identity. This being the case, the original BIF interpretation should be considered viable until more definitive evidence (perhaps oxygen isotopes) becomes available.

J. MICHAEL PALIN
Department of Geology, University of Otago, Post Office Box 56, Leith Street, Dunedin 9001, New Zealand. E-mail: michael.palin@stonebow.otago.ac.nz

Response

OUR STUDY INTEGRATED (i) DETAILED structural observations, (ii) mineralogy, (iii) geochemistry, and (iv) regional geologic events for interpreting rocks that have been repeatedly deformed and metasomatized over approximately 2 billion years. Palin questions our proposed metasomatized ultramafic igneous origin for quartz-pyroxene rocks on Akilia solely on the basis of assessment of a few geochemical ratios that overlap the field of Isua banded iron formation (BIF) (see Fig. 3A), suggesting that they support previous claims (*1*, *2*) for a BIF protolith.

We are not surprised by the broad compositional range in Cr/Th versus Th/Sc or TiO_2 versus P_2O_5 for the quartz-pyroxene rocks and pyroxenite boudins, considering that metasomatic quartz (and likely carbonate) has diluted their original ultramafic composition by in excess of 90% in some samples. In addition to overlapping the field of

Image not available for online use.

The rocks under discussion.

CREDIT: C. FEDO/GEORGE WASHINGTON UNIVERSITY